Transmission Techniques for Radio LAN's—A Comparative Performance Evaluation Using Ray Tracing

Aram Falsafi, Kaveh Pahlavan, *Fellow, IEEE*, and Ganning Yang, *Member, IEEE*

Abstract— **This paper uses the results of ray tracing in a typical indoor test area to compare the performance of major radio transmission techniques that are used as the air interface in evolving standards and major wireless local area network (WLAN) products. The performance of direct sequence (DS) and frequency hopping spread spectrum (FHSS) in the test area are compared with the performance of multicarrier modems, as well as modems using decision feedback equalization (DFE) and sectored antenna systems (SAS). The validity of using ray tracing for performance evaluation is examined by comparing the results with the results of performance evaluation obtained from the empirical measurement of the channel characteristics. Based on the maximum achievable data rate and minimum power requirement determined in the test area, operation of all modems in bandlimited and power limited applications are discussed.**

I. Introduction

WIRELESS local area networks (WLAN's) are designed for local high speed wireless communication among computer terminals. A typical WLAN supports a limited number of users in a well-defined local area and the existence of a standard is not crucial for the development of products. As a result, while the access methods and network topologies used in WLAN's are much the same from one system to another, a variety of radio and infrared (IR) transmission technologies have been examined for different WLAN products [1]–[4]. This paper provides a quantitative comparative study among various radio transmission techniques used for implementation of WLAN's. To develop the analysis, a ray tracing algorithm is used to simulate the radio channel for a typical indoor area considered as a test site for WLAN operation. Although we do not expect drastic disparities for any other indoor area, the reader is encouraged to find other buildings that may result in different conclusions.

The concept of a WLAN was first introduced at the beginning of the 1980's [5], [6]. In the middle of that decade, industrial, scientific, and medical (ISM) bands were released in the United States [7]–[9] and various approaches for implementation were examined [1]. The first WLAN products appeared in the market around 1990 [10]–[14] and IEEE 802.11 standards started shortly after that [15]–[17]. Today, a variety of technologies and several sectors of the market have been examined for WLAN's, and major international standards are evolving.

The IEEE 802.11 committee and the European Telecommunications Standards Institute (ETSI) RES-10 committee for HIPERLAN are developing standards for physical and MAC layers of WLAN's. At the same time, WINForum is developing an etiquette for wireless high speed local communications in the unlicensed personal communication system (PCS) bands. IEEE 802.11 is focusing on operation in the ISM bands that are restricted to spread spectrum technology. Radio LAN's in the ISM bands either use direct sequence spread spectrum (DSSS) or frequency hopping spread spectrum (FHSS). The ETSI's RES 10 considered decision feedback equalization (DFE), multicarrier modulation (MCM), and sectored antenna systems (SAS) for the HIPERLAN, finally deciding on DFE [18]–[20]. That leaves five major transmission techniques (DSSS, FHSS, DFE, MCM, and SAS) for radio LAN's. A variety of manufacturers have used or are examining these technologies in their products.

The market for WLAN's is evolving around the following five categories of applications [4]:

- LAN extension,
- nomadic access,
- *Ad hoc* networking,
- inter-LAN bridges, and
- fusion of computer and communications.

The first three applications are traditional applications. The point-to-point inter-LAN bridges are an emerging successful market for WLAN's. The last application is being examined by the research community and is in its exploration phase. All these applications are mainly considered for indoor areas except the inter-LAN bridges that are often used outdoors to interconnect LAN's in separate buildings.

The major technical issues for the WLAN's are:

- data rate,
- coverage,
- power consumption and size,
- interference (inter-operability and coexistence),
- protocols, and
- security.

The first four issues are related to transmission technology and the last two are networking issues. The data rate is the most important technical factor in the wired LAN industry and it is a function of the transmission technology and the media for

Manuscript revised November 1, 1995. This paper was presented at the Personal, Indoor and Mobile Radio Communications Conference (PIMRC'95), Toronto, Canada, September 27–29, 1995.

A. Falsafi and K. Pahlavan are with the Center for Wireless Information Network Studies, Worcester Polytechnic Institute, Worcester, MA 01609 USA.

G. Yang is with Rockwell Telecommunications, Long Beach, CA USA.

Publisher Item Identifier S 0733-8716(96)01905-1.

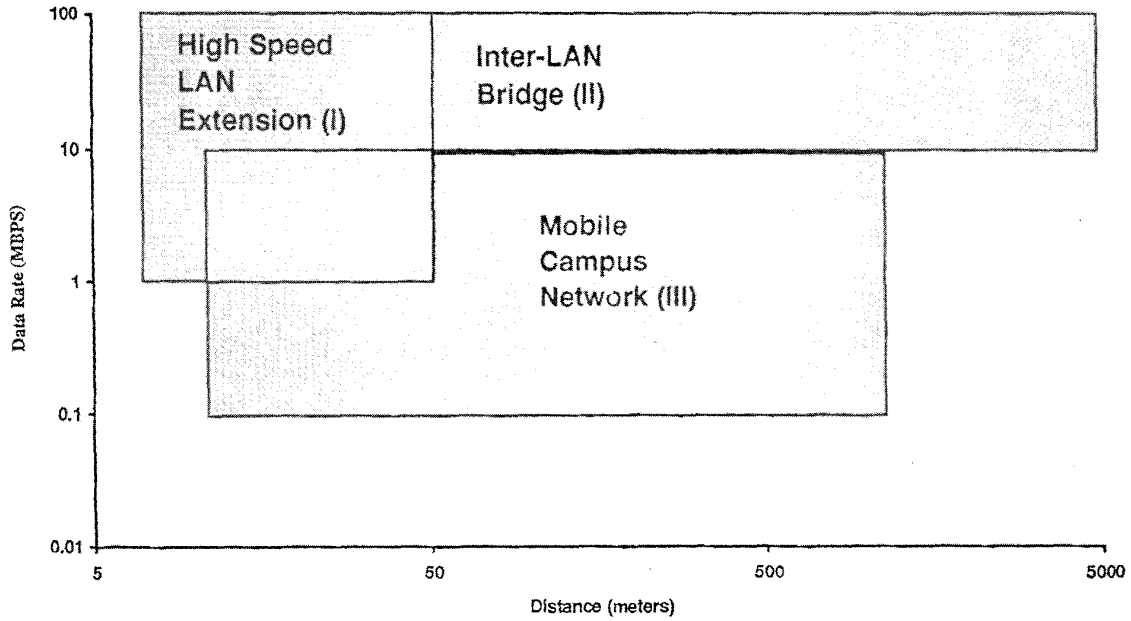

Fig. 1. Coverage and data rates for three classes of WLAN applications.

communication (twisted pair, cable, or fiber). The media for communication for the WLAN industry is the air. However, transmission technology, availability of and restrictions on the band, as well as the frequency of operation, govern the data rate. These factors also affect the coverage and power/size requirements that change from one application to another. The main issue for a WLAN manufacturer that desires to approach a certain market is evaluation of various transmission technologies within the available bands in terms of supportable data, coverage, and power/size requirements. These issues are addressed in this paper. The interference in WLAN's is addressed in [21] and [22]. In its simplest form, designers can extend existing wired protocols to WLAN's. For a mobile user who would like to receive continuity of service while changing the wireless access point, the protocols should be modified to manage mobility. Issues related to the mobility management in WLAN's are addressed in [23]–[25]. Since wireless information is transmitted through broadcast over the air, naturally, the user will feel less secure than in the wired system. Work in this area is addressed in [26].

Figure 1 relates the coverage and data rate to three classes of wireless local services. The first class of services covers distances of less than 50 m. These services are the focal point of the standards activities and are the most common form of what we refer to as a WLAN. This class includes stationary first generation high speed WLAN's as well as PCMCIA cards designed for mobile laptops. For the services provided to stationary terminals, the most important issues are the data rate and coverage. For the mobile services provided to laptops, size and power consumption also come into the picture. To expand the size of the market, most first generation stationary WLAN manufacturers have added directional antennas and have maximized the transmission power to market their products as point-to-point inter-LAN bridges. Wireless inter-LAN bridges operate between buildings and in most applications in a line-of-sight (LOS) connection. The range of these products is on the order of a kilometer. The third class of services are evolving around campus environments. The purpose of this class of applications is to provide a WLAN service that covers an area the size of a campus. The key issue for this sector of the industry is the availability of PCMCIA interface cards, power consumption, and coverage. The data rate is essential as usual, although a service of this sort even with a data rate of a few hundred kilobits per second is expected to find a substantial market.

The remainder of this paper is organized as follows. Section II addresses the selection of a channel model for an accurate performance evaluation for transmission techniques used in WLAN's. Section III describes the signal processing models that are used for various transmission techniques considered in this paper. Section IV examines the accuracy of the results of ray tracing, analyzes the effects of various transmission parameters, and provides a comparative performance evaluation among all five transmission techniques in a test area. Finally, conclusions are presented in Section V. The Appendix provides the equations that are used for calculation of the error rate for different techniques.

II. Channel Modeling

The objective of analytical performance prediction of wideband transmission techniques is to develop a set of mathematical equations that calculate the probability of error or the probability of outage of a transmission technique for a modeled wideband channel characteristic. The most popular mathematical model for describing wideband characteristics of the channels is the so-called discrete multipath time-domain model. It was developed by Turin to describe propagation in the urban radio channel [27] and was later applied to the indoor

radio channel [28]–[31]. This model describes the channel as a linear time-invariant filter whose impulse response is the sum of L paths with the lth path having three parameters, amplitude, β_l, delay, τ_l, and phase, φ_l

$$h(t) = \sum_{l=0}^{L-1} \beta_l \cdot \delta(t - \tau_l) \cdot e^{j\phi_l} \tag{1}$$

where $\delta(\cdot)$ is the Dirac delta function.

There are three approaches to determining the path parameters of a channel described by the above equation: 1) using the results of field measurements, 2) assuming a statistical model for the parameters, and 3) using site-specific computer simulation techniques such as ray tracing or finite difference time domain (FDTD) [32]. Results of wideband indoor radio measurements have been examined for performance evaluation of DFE [33], [34], and DSSS [35]. The major problem with this approach is that the collection of a large set of wideband measurements in a site is very expensive and time consuming—the measurement procedure will need to be repeated to evaluate the performance in a new area. As a result, measurements are usually used to support the accuracy of statistical or building-specific channel models that can be extended to other areas more economically.

There are a variety of statistical models with different levels of complexity that are used for performance evaluation of systems operating in indoor radio channels. The simplest models determine the number of paths from the value of the root-mean-square (rms) delay spread of the channel and assume all paths are Rayleigh fading with equal strength. These models have been used in performance predictions of DSSS systems [36]. Most of the time, simple statistical models do not provide very accurate results [32]. More complex statistical models extract parameters of (1) from direct wideband measurements of the channel [28]–[30], [37], [38]. These models are suitable for urban radio environments and are adopted by most cellular telephone and PCS standards [32]. The statistical indoor radio channel model developed in [28] has been used for performance evaluation of modems with equalizers [39], [40]. The weakness of using statistical indoor models for WLAN applications is that they do not relate propagation to the specific layout of a building.

Site-specific computer simulation techniques provide a cost efficient and comprehensive solution to the indoor radio channel modeling problem. These models use the floorplan of the building as the boundary to solve radio propagation equations in a typical indoor area. Once the software is developed, generation of a new set of profiles in a new building does not incur any additional cost. The two main approaches to solving the radio propagation equations are ray tracing and FDTD. With today's computational facilities, the implementation of FDTD for WLAN applications is not yet as attractive as the ray tracing algorithm [32]. Besides, ray tracing can also provide direction-of-arrival information, which is necessary for an accurate analysis of the performance of modems using SAS. As a result, we use a ray tracing algorithm to determine the channel characteristics for our comparative performance evaluation studies. The rms delay spreads obtained by ray tracing are usually smaller than the corresponding values obtained from the results of measurements [41], [42]. Since it is a common belief that the maximum data rate is proportional to the inverse of the rms delay spread, one may question the accuracy of the data rate limitations obtained by using a ray tracing program. To examine the accuracy of the results of performance evaluation using the ray tracing algorithm, we compare the results with the results of extensive measurements in a typical indoor area suitable to WLAN applications.

The two most popular techniques for implementing ray tracing are known as ray shooting and the image method. In ray shooting, rays are sent out from the transmitter at small incremental angles (usually every few degrees) and are followed until they either attenuate below a certain threshold or intersect with the receiver. In the image method, the transmitter's image is repeatedly reflected through the surfaces, which are treated as mirrors. It is then possible to determine which reflections of the transmitter are visible from the receiver [43]. The disadvantage of the image method is that the number of paths grows exponentially with the number of reflecting surfaces and with the number of reflections. Therefore, very little detail can be incorporated into the floorplan before the computational requirements of the program become unreasonably large. Lebherz *et al.*, have developed a three-dimensional ray tracing environment for cellular and micro-cellular applications [44]. Other ray tracing techniques for indoor applications are reported in [45]–[47]. The details of the ray tracing program used in this paper can be found in [42], [48]. This ray tracing program uses the ray shooting algorithm described earlier.

For the purpose of this study, the second floor of Atwater Kent Laboratories at Worcester Polytechnic Institute was used to represent the test area considered as a typical indoor environment suitable for WLAN operation. The floorplan of the center section of the second floor is shown in Fig. 2. The locations of the transmitter and receiver used for measurements and ray tracing are marked on the floorplan. To simulate small variations in channel characteristics caused by local movements of terminals, as well as movement of people or objects around the terminals, random phase was added to the path arrivals at each receiver location. The resulting impulse responses provided sufficient channel profiles for performance evaluation simulation reported in this study. As shown in [42], the cumulative distribution function (CDF) of the rms delay spread of the simulated channel and the results of measurements are significantly apart. The average rms delay spreads for the simulation and the measurements are 19.6 and 23.2 ns, respectively. Some results of comparative performance evaluation of DFE and SAS in this test area were reported in [42]. This paper provides a much larger perspective that analyzes the performance of DFE and SAS, as well as DSSS, FHSS, and MCM in bandlimited and power limited conditions.

III. Signal Processing Models for Transmission Techniques

This section describes the system structure and the signal processing details of the five transmission techniques that are

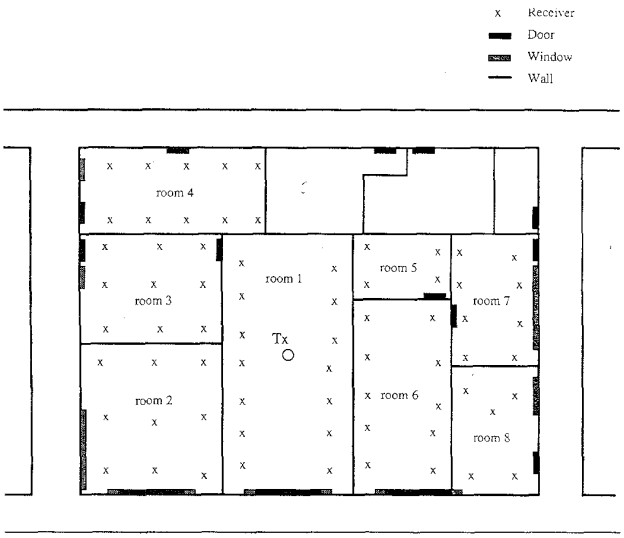

Fig. 2. Center section of the second floor of Atwater Kent Laboratories at Worcester Polytechnic Institute.

considered for WLAN's, from the information source up to the sampling before the decision process. The method for calculation of the error rate of the coded and uncoded systems using these sampled signals is straightforward and is described in the Appendix. We divided the transmission techniques into two classes: spread spectrum systems (DSSS and FHSS) that are considered by the IEEE 802.11 committee and other systems (MCM, DFE, and SAS) that were considered by ETSI's RES-10 for HIPERLAN and are also suitable for evolving unlicensed PCS band products. The modulation technique considered for all transmission systems is quantenary phase shift keying (QPSK) with coherent detection.

For a QPSK modulation, the complex data symbol, b_i consists of two information bits and can take values $\pm 1 \pm j$. At the transmitter, data is modulated onto the in-phase (I) and quadrature phase (Q) channels of a carrier. The signal is then passed through the modulator and transmitted over the channel, where it is distorted by the channel multipath characteristics and additive white Gaussian noise (AWGN). The channel multipath characteristics are derived for different placements of the transmitter and receiver. At the receiver, the signal is demodulated, processed, and sampled at the time determined by the timing recovery circuit. The resulting decision variable is phase-compensated and used to determine the bits transmitted over the I and Q channels.

A. Spread Spectrum Systems in ISM Bands

The DSSS technology was first suggested for wireless terminals in 1980 [6] and WLAN using spread spectrum technology was one of the main applications considered for the release of ISM bands [4], [7]–[9]. Today, DSSS WLAN's have been sold more than any other WLAN technology and many companies are developing DSSS and FHSS products on PCMCIA cards. The IEEE 802.11 is developing standards for DSSS and FHSS systems operating in ISM bands [4]. WLAN users need the entire capacity of the channel for quick transmission of data bursts generated by each terminal and code-division multiple-access (CDMA) is not suitable for that situation [12]. As a result, CDMA is not considered by IEEE 802.11 and it is not used in any of the major products in the market. However, some WLAN manufacturers assign several codes to an individual user to increase the data rate while still operating under ISM band restrictions. They refer to this technology as CDMA-based WLAN technology. The reader should note that this is not the CDMA technology as used in the cellular telephone industry.

1) Model for DSSS: The DSSS system that we used in this analysis is assumed to have a spreading gain of N and chip period T_c, such that $T = N \cdot T_c$ is the symbol period. The spreading signal at the transmitter is given by

$$x_t(t) = \sum_{n=0}^{N-1} a_n \cdot p(t - nT_c) \tag{2}$$

where $\{a_n\}$ is the pseudo-noise (PN) spreading sequence and $p(t)$ is a wave pulse of duration T_c. The transmitted baseband signal is thus given by

$$\begin{aligned} s(t) &= \sum_i b_i \cdot x_t(t - iT) \\ &= \sum_i \sum_{n=0}^{N-1} b_i \cdot a_n \cdot p(t - iT - nT_c). \end{aligned} \tag{3}$$

The received signal is the convolution of $s(t)$ with the channel impulse response given by (1), plus additive noise

$$\begin{aligned} r(t) &= \sum_{l=0}^{L-1} \beta_l \cdot s(t - \tau_l) \cdot e^{j\varphi_l} + n(t) \\ &= \sum_i b_i \left\{ \sum_{n=0}^{N-1} a_n \right. \\ &\quad \left. \cdot \left[\sum_{l=0}^{L-1} \beta_l \cdot p(t - \tau_l - iT - nT_c) \cdot e^{j\varphi_l} \right] \right\} + n(t). \end{aligned} \tag{4}$$

The receiver filter is matched to the PN sequence, such that the cross-correlation of the transmitted signal and the periodic despreading signal has a peak centered at zero delay

$$\begin{aligned} R_x(\tau) &\equiv \int_{-\infty}^{\infty} x_t(t) \cdot x_r(t + \tau) \cdot dt \\ &= \begin{cases} N - \dfrac{2 \cdot |\tau|}{T_c}, & \text{for } |\tau| < \dfrac{T_c}{2} \\ -1, & \text{for } \dfrac{T_c}{2} \le |\tau| \le T \\ 0, & \text{for } T < |\tau|. \end{cases} \end{aligned} \tag{5}$$

Using the above definition, the receiver's despreader output is given by

$$z(t) = \sum_i \sum_{l=0}^{L-1} b_i \cdot \beta_l \cdot R_x(t - iT - \tau_l) \cdot e^{j\phi_l} + n_1(t) \tag{6}$$

where $n_1(t)$ is the front-end filter's response to AWGN. In this paper, we study RAKE receivers with up to four taps. The receiver samples $z(t)$ at up to four highest peaks, which are detected using a sliding window. It then phase-compensates

the complex sample to yield the decision variable. The receiver uses a maximal-ratio combiner; the tap outputs (including noise power) are multiplied by the estimate of channel gain at the corresponding sample times and added to yield one decision variable that is used for the calculation of error rate using equations described in the Appendix.

2) Model for FHSS: In the frequency hopping system considered in this paper, the transmitter and receiver pulse-shaping filters, $g_t(t)$ and $g_r(t)$, respectively, are identical with a square root raised cosine frequency response with rolloff factor α. In order to make the baseband representation simple, we treat all hops as offsets from the lowest carrier. The carriers are assumed to be equally spaced with the nth carrier given by $f_n = f_0 + (\Delta f) \cdot n$ and Δf being the separation between carriers. The baseband representation of the transmitter output, conditioned on carrier index n, is therefore given by

$$s(t|n) = \sum_i b_i \cdot g_t(t - iT) \cdot e^{j2\pi \cdot \Delta f \cdot n \cdot t} \tag{7}$$

where $\{b_i\}$ is the complex data sequence. The received signal is obtained by convolving $s(t)$ with the channel impulse response and adding noise. This is then de-hopped and passed through the receiver's matched filter, yielding

$$z(t|n) = \sum_i \sum_{l=0}^{L-1} b_i \cdot \beta_l \cdot g(t - iT - \tau_l) \cdot e^{j(2\pi \cdot \Delta f \cdot n \cdot \tau_l + \phi_l + \theta_n)} + n_1(t) \tag{8}$$

where θ_n is the phase offset between the frequency hopping (FH) modulator and demodulator and $g(t)$ is the impulse response of a raised-cosine pulse shaping filter as obtained by convolving $g_t(t)$ with $g_r(t)$. Finally, $z(t)$ is sampled and phase-compensated, yielding a decision variable conditioned on hop carrier n. The sampling time is obtained following the practical method derived in [49]. The error rate for each hop is then calculated from the corresponding decision variable. Assuming that the occurrence of all hops are equally likely, the aggregate error probability without coding would be the average of the error probabilities at each hop. The effects of coding on the error rate calculation are discussed in the Appendix.

B. HIPERLAN and Other Transmission Techniques

Other bands considered for WLAN development are the bands assigned to ETSI's RES 10 for development of standards for HIPERLAN, the PCS unlicensed bands, and some licensed bands used, in particular, for wireless inter-LAN bridges. Spread spectrum is not a requirement in these bands and other technologies such as DFE, MCM, and SAS, as well as spread spectrum technology, can be considered. Similar to spread spectrum technology, all these techniques can mitigate the effects of multipath. Samples of the analysis of these systems are available in [50]–[53].

Considerable discussion in the RES 10 has been carried out to examine the effectiveness of all transmission technologies for the implementation of the 20 Mb/s HIPERLAN. Developments in the unlicensed PCS bands are premature, but they will most probably be affected by decisions made on HIPERLAN. In the RES 10, spread spectrum CDMA has not been selected for two reasons: 1) Given the target user data rates and the available system bandwidths for HIPERLAN, the processing gain of a CDMA system would be impractically small. 2) Efficient CDMA is only possible in a star topology that is essential for the implementation of power control, but HIPERLAN is chartered for other topologies as well [19]. As mentioned earlier, another important factor is that CDMA is not suitable for quick transmission of bursts of data that demand the full capacity of the transmission medium. Without CDMA, spread spectrum sacrifices the bandwidth to provide superior coverage. The superior coverage of spread spectrum technology is due to the anti-multipath and anti-interference nature of this technology and is a function of the spreading factor of the system.

Some of the pioneering WLAN products in the market are using sector antenna technology for operation in the licensed bands [10]. Also, the possibility of using sectored antennas in HIPERLAN has been addressed in the RES-10. To accommodate mobile terminals with HIPERLAN specifications, these antennas would need to be switched beam or steerable and it was felt that the control of such antennas would be difficult to manage in a mesh topology network. Furthermore, directive gain can only be achieved with significant aperture (in terms of wavelengths), which would result in physically large antennas at HIPERLAN frequencies [19].

The DFE and MCM were subject of the most lengthy discussions in the RES 10. The general feeling in the RES-10 was that although the advantages of MCM were recognized, the disadvantages had not been thoroughly investigated and hence this would be a high risk solution to the time dispersion problem for HIPERLAN. Ultimately, the decision was taken to reject the multicarrier transmission scheme and accept a single carrier/equalizer transmission scheme for HIPERLAN. It was the general feeling in RES-10 that the DFE was a good compromise between complexity and performance. Although the equalizer design would not be specified in the standard, the standard must be written around a feasible approach. The exact specification of the equalizer depends on the modulation scheme chosen [19].

1) Model for MCM: The overall format of the equations used for the analysis of the multicarrier system is the same as those used for the frequency hopping system. However, depending on the frequency separation between carriers, interference from adjacent carriers may also need to be taken into account. This analysis is applicable to all implementations of MCM, including orthogonal frequency division multiplexing (OFDM) [51], [53], [54]. Given reasonable pulse shaping filters, every carrier will only be interfered with by its two adjacent carriers. If b_i^n is the information symbol carried by the nth carrier during the ith symbol interval, the corresponding decision variable can then be written as

$$\begin{aligned} z(t|n) &= \left\{ \sum_i \sum_{m=-1}^{1} b_i^{n+m} \cdot g_t(t - iT) \cdot e^{j(\Delta\omega)m \cdot t} \right\} \\ &\quad * h(t) * g_r(t) + n_1(t) \\ &= \sum_i \sum_{m=-1}^{1} b_i^{n+m} \cdot e^{j(\Delta\omega)m \cdot i \cdot T} \cdot r_m(t - iT) \end{aligned} \tag{9}$$

where

$$r_m(t) = \sum_{l=0}^{L-1} \beta_l \cdot e^{j\phi_l} \cdot g_m(t - \tau_l)$$

and

$$g_m(t) \equiv \int_{-\infty}^{\infty} g_t(\tau) \cdot e^{j(\Delta\omega)m\cdot\tau} \cdot g_r(t - \tau) \cdot d\tau$$

$g_0(t)$ is simply a raised cosine pulse, equal to $g(t)$ used in the frequency hopping model above. Expressions for $g_m(t)$ for $m = \pm 1$ were presented in [54].

When using multicarrier modulation, it is important to provide an adequate "guard band" between the carriers. The time-bandwidth product is defined as the product of symbol period T and frequency separation Δf, and can be viewed as the inverse of bandwidth efficiency. If the total system bandwidth and number of carriers are fixed, increasing the time bandwidth product will reduce the amount of interference from adjacent carriers, at the expense of data rate. Given that $\alpha = 0.5$ is a popular design choice, a time-bandwidth product of 1.5 was found to provide sufficient separation between carriers. This was used throughout the simulations presented in this paper.

2) Models for DFE and SAS: The model used for performance analysis of the DFE and SAS closely follows those reported in [42]. When sectored antennas are used, the channel impulse response for each antenna sector is modified to take into account the direction of arrival of each path. This analysis assumes that the receiver is equipped with a six-sector directional antenna whose polarizations are vertical. The ith antenna pattern is defined by the function

$$g_i(\psi) = \begin{cases} \dfrac{\sin\left(\dfrac{2.78 \cdot \dfrac{\psi - \pi i}{3}}{\Phi}\right)}{\dfrac{2.78 \cdot \dfrac{\psi - \pi i}{3}}{\Phi}}, & \text{for } \dfrac{\pi i}{3} - \dfrac{\Phi}{2} \le \psi < \dfrac{\pi i}{3} + \dfrac{\Phi}{2} \\ a_0, & \text{otherwise} \end{cases}$$

where $g_i(\psi)$ is the normalized power gain for a ray arriving from angle ψ and Φ is the 3 dB beamwidth of the antenna which is set to $\pi/3$, resulting in six sectors. The channel impulse response for the ith sector is, therefore, given by

$$h_i(t) = \sum_{l=0}^{L-1} \beta_l \cdot \delta(t - \tau_l) \cdot e^{j2\pi\phi_l} \cdot g_i(\psi_l) \qquad (10)$$

where ψ_l is the angle of arrival of the lth path. Equation (8), used for FHSS with one hop, and (10) for the channel impulse response, are used to evaluate the decision parameter for a sector of the antenna. The sector associated with the maximum received signal power is selected for communication over the channel. These signal powers are determined by calculation of average received power in all six sectors for each individual channel profile and are reflected in the plots of achievable data rate.

In the case of DFE modems, the value of the taps for each channel profile is obtained by solving the set of linear equations that are obtained from the minimization of the mean error between the equalized sample and the desired detected sampled value. The overall sampled impulse response after equalization is then used as the decision variable in the calculation of the error rate. The details of derivations for the taps of the equalizer and the overall impulse response are available in [50]. The DFE used in our analysis has three forward and three feedback taps that provide effective and practical solutions to the problem [34].

IV. Results of the Analysis

In this section, we first examine the validity of performance evaluation using the impulse responses generated from ray tracing by comparing the results with those generated from the empirical data on the wideband channel characteristics. Then, performance of different transmission techniques in our indoor test area will be examined and the effects of receiver complexity on the performance will be analyzed. Finally, a comparison among all transmission techniques operating in the test area is presented.

A. Validation of the Ray Tracing Approach

Results of 680 wideband (200 MHz) frequency domain measurements at 1 GHz in the second floor of Atwater Kent Laboratories at Worcester Polytechnic Institute were used for performance evaluation using the empirical data. The details of the measurement system and the characteristics of the results are described in [37]. The floor plan of the same area, same locations for transmitter–receiver pairs, and the same center frequency were used as input to the ray tracing program to generate the performance predictions based on the ray tracing.

One set of performance evaluation curves often used in the literature is the plot of probability of error averaged over all measured wideband channel characteristics as a function of the transmitted power. These plots are used for calculation of the minimum transmission power needed to achieve a certain error rate. Fig. 3 is a plot of average error probability versus transmitted power for MCM with 31 carriers. The system bandwidth was set to 25 MHz and the error probability is plotted as a function of total transmitted power. The bandwidth used by each carrier was 1.5 times the symbol rate, resulting in a bandwidth efficiency of 0.67. As can be seen from the plot, impulse responses generated by ray tracing and those collected through measurements result in error probability estimates that are very close. Similar plots for DSSS, FHSS, DFE, and SAS were examined and in all cases the results obtained by ray tracing and those from the empirical data showed close agreement.

It is often desirable to view a data channel as on/off, where outage is defined as the bit error rate exceeding a certain threshold. Outage probability can then be defined as the percent of time that a given location is in outage or the percent of locations that are in outage at a given time. The former is often used to describe time-varying channels such as urban mobile, while the latter is used to describe fixed installations such as indoor WLAN's. In a fixed bandwidth

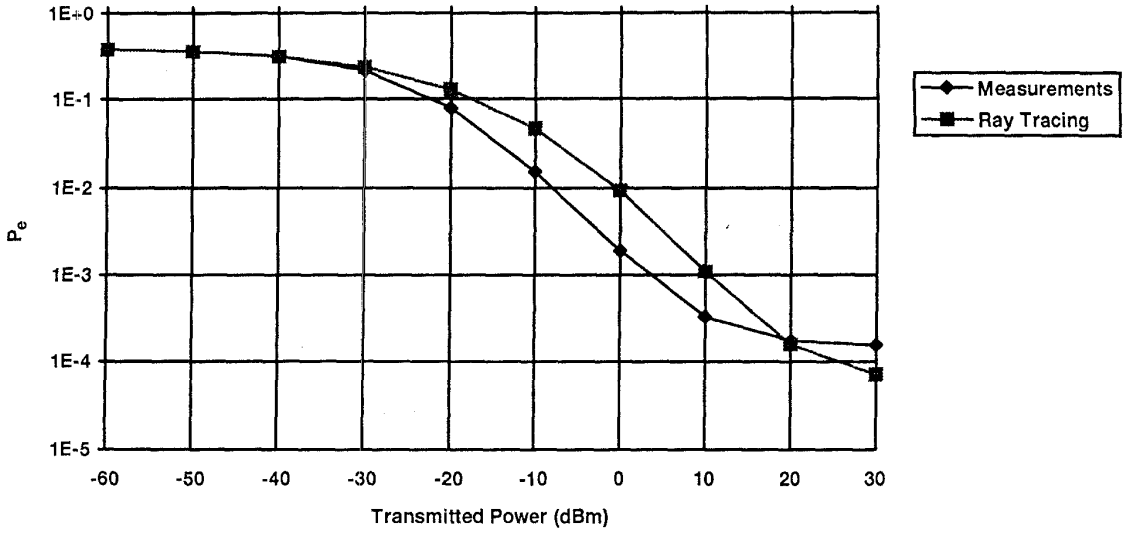

Fig. 3. P_e versus transmitter power, MCM-31, 25 MHz.

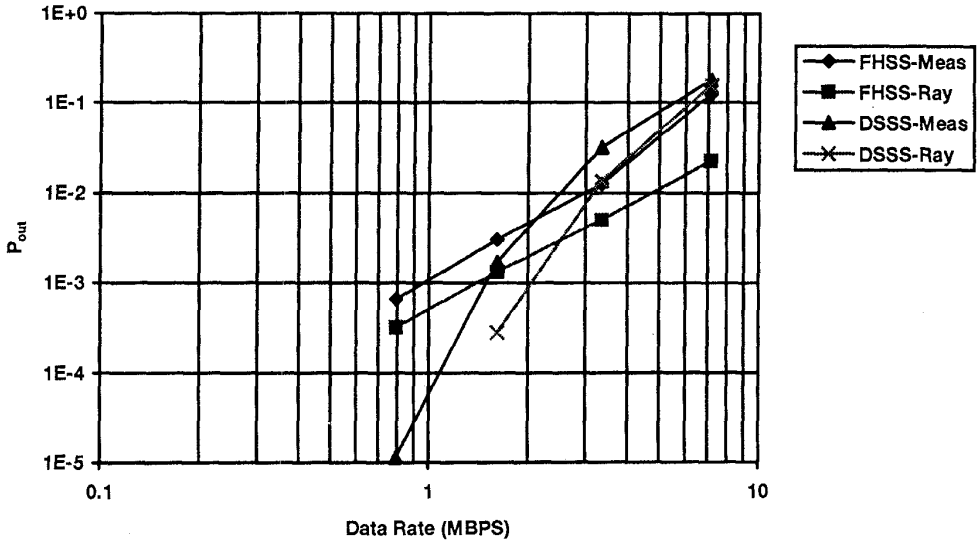

Fig. 4. P_{out} versus data rate, spread spectrum, 25 MHz, 100 mW.

of 25 MHz, processing gains of 7, 15, 31, and 63 result in data rates of approximately 3.57, 1.67, 0.807, and 0.397 Mb/s, respectively, for both DSSS and FHSS. Fig. 4 shows the probability of outage versus data rate for the DSSS and FHSS systems, where outage is defined as the bit error rate (BER) exceeding 10^{-5}. The transmitted power is 100 mW and the bandwidth is 25 MHz. Again, it can be observed that ray tracing produces channel impulse responses that can be used instead of the results of direct wideband measurement in the prediction of error rate. Similar plots were generated for other modulation techniques and the conclusions remained the same. Other plots that evaluated the probability of error versus data rate and other technical parameters were examined for the two sets of channel profiles and results were always very close.

It can, therefore, be concluded that the impulse responses generated through ray tracing result in error probability estimates that are comparable to those obtained from direct measurements. Later in this paper, ray tracing results will be used to compare the performance of different transmission techniques proposed for wireless local area networks at different levels of system complexity.

The average rms delay spreads from the results of the ray tracing and the empirical data in our test area are 19.6 and 23.2 ns, respectively. The results of ray tracing often show lower values of the rms delay spread when compared with empirical data [32], [41], [42]. The simple approximated rules for evaluation of maximum data rate of a transmission technique are all developed around the inverse of the rms delay spread [32]. Therefore, the discrepancies between the values of rms delay spread obtained from ray tracing and empirical data suggests significant differences in the estimate of the maximum supported data rate. This conclusion is in contrast to all the cases that we have reported above and the situation can be explained as follows.

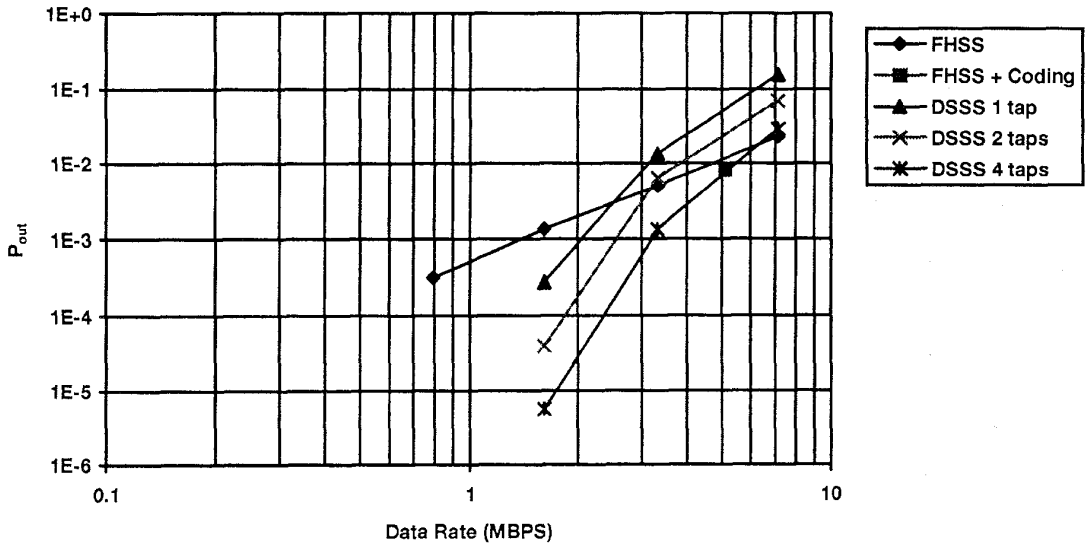

Fig. 5. P_{out} for spread spectrum with different levels of system complexity, 25 MHz, 100 mW.

The discrepancies among the rms delay spread values obtained from ray tracing and the empirical data are caused by very weak paths at large arrival delays that usually appear in the results of measurements but not in the results of ray tracing. The square of the delay spread is involved in calculation of the rms delay spread, magnifying the impact of these paths. In performance prediction of different wideband modulation techniques, however, these paths cause very small intersymbol interference (ISI) that has a negligible effect on the error rate of the system. The important issue is that ray tracing predicts the major paths very closely and these paths are the ones that affect the performance. This discussion warns those using rms delay spread as an absolute measure for classification of the channels. In reality, rms delay spread is an excellent parameter representing the wideband characteristics of the channel if there are not many weak paths arriving at large delays. Another related important issue is that during measurements, noise peaks or other artifacts are often mistaken for weak paths at large delays [32], [55] and the actual existence of these paths is questionable. Considering the discussion presented here, we may state that rather than looking into the results of ray tracing and claiming that they provide low rms delay spreads, we may state that the result of rms delay spreads obtained from the measurements often provide pessimistic values. To decrease these values we can simply raise the threshold used for detecting the peaks.

B. Effects of System Complexity

We have introduced various transmission technologies and have described the mathematical models for the analysis of the systems. We showed the accuracy of the ray tracing algorithm to be used for the performance evaluation of WLAN's. Now we examine the results of simulations to determine the effects of various transmission parameters on the performance of each transmission technique. We start with spread spectrum systems and then we examine MCM, DFE, and SAS.

When combined with a RAKE receiver, DSSS provides sufficient resolution to allow individual paths to be extracted from the received signal, providing a form of time diversity. FHSS, on the other hand, can take advantage of the fact that in a frequency selective fading channel different portions of the spectrum tend to fade independently. Significant improvements can be achieved with a small reduction in data rate through the use of channel coding and interleaving that take advantage of the frequency diversity embedded in this modulation technique. We provide some quantitative results to address the effectiveness of time- and frequency-diversity in DSSS and FHSS, respectively.

Figure 5 is a plot of outage probability for an outage threshold of 10^{-5} as a function of data rate for FHSS with and without Reed–Solomon coding, and DSSS with RAKE receivers applying maximal ratio combining to the outputs of the fingers of the RAKE receiver. The transmitted power is kept at 100 mW (a reasonable value to cover our test area) and the transmission bandwidth is 25 MHz, which is close to what is used by the IEEE 802.11 standard for spread spectrum communication. Block coding has been considered in conjunction with the FHSS system. Reed–Solomon codes of (7, 5), (15, 11), (31, 23), and (63, 45) are assumed, resulting in data rates of 2.55, 1.22, 0.60, and 0.28 Mb/s.

As we increase the data rate in a fixed band with constant transmission power, the performance of DSSS deteriorates faster than that of FHSS without coding. At the outage rate of 1%, the FHSS and the DSSS with more than two-tap RAKE receivers can provide a data rate of 2 Mb/s, i.e., the target value for IEEE 802.11. Going from a one-tap to a four-tap RAKE receiver, the data rate can be increased almost two times. When coding is used with FHSS, the outage rate for data rates below 2 Mb/s is almost zero, providing a robust coverage of the area.

As we discussed earlier, the mathematical analysis of MCM is very similar to that of FHSS. In FHSS, a narrowband signal

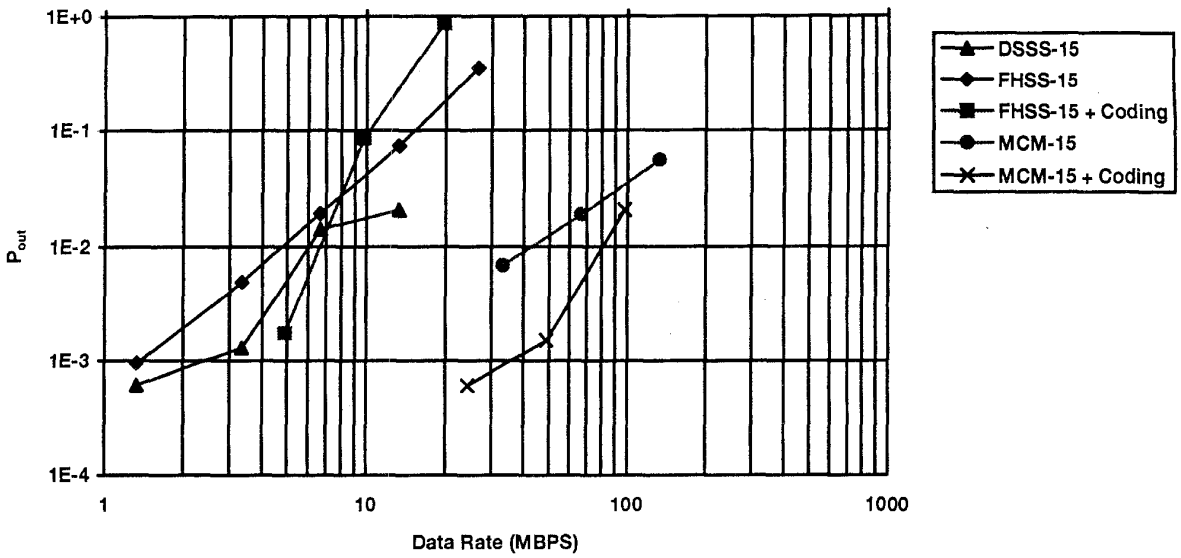

Fig. 6. P_{out} versus data rate, unlimited bandwidth, 100 mW.

hops over different carrier frequencies, while in MCM all carriers simultaneously transmit a narrowband signal. We can control the multipath with both techniques by reducing the bandwidth of the signal modulated over individual carriers to values well below the coherence bandwidth of the channel. Coding results in significant performance improvement in both systems by taking advantage of the inband frequency-diversity of the channel. Reduction in the bandwidth of individual carriers in MCM increases the number of carriers within a fixed transmission bandwidth. This adds to the complexity of the system, but it does not change the data rate. The same situation for a FHSS system results in reductions in the bandwidth of the individual carrier and transmission rate, and an increase in the processing gain of the system, improving the coverage. Fig. 6 presents the probability of outage versus data rate for FHSS and DSSS systems with a processing gain of 15, and MCM with 15 carriers for an unlimited available bandwidth and a 100 mW transmission power. An MCM system provides a higher data rate, but permits only one user in the band. DSSS and FHSS, on the other hand, could allow several users to share the band simultaneously using CDMA.

Figure 7 shows the minimum power requirement versus number of carriers for an MCM system operating in a 25 MHz bandwidth. The performance is considered to be acceptable if the outage rate is 1%. With a time-bandwidth product of 1.5, used in this paper, a system bandwidth of 25 MHz and 7, 15, 31, and 63 carriers resulted in data rates of 17.5, 17, 16.8, and 16.7 Mb/s, respectively. With coding, the data rates are reduced to 12.5, 12.1, 12.4, and 11.9 Mb/s, respectively. For an MCM system operating in a fixed bandwidth, the overall data transmission rate remains independent of the number of carriers. However, as the number of carriers is reduced both transmission power and bandwidth of individual carriers increases linearly. As long as the bandwidth of each carrier is well below the coherence bandwidth of the channel, the channel is flat fading. The increase of the bandwidth of individual carriers allows more additive noise into the receiver front end. The effects of this noise are compensated for by the increase in the transmission power due to reduction in the number of carriers resulting in no changes in the signal-to-noise ratio (SNR) and consequently the error rate of the modem. In this situation, the least complex design is the one that uses the minimum number of carriers. As the number of carriers reduces below a certain number, around 15 in Fig. 7, the bandwidth of the individual carriers gets close to the coherence bandwidth of the channel, the channel becomes frequency selective and ISI causes additional degradation. In this situation the performance is no longer independent from the number of carriers. Therefore, for an MCM system operating in a frequency selective channel there is always an optimum number of carriers that minimizes the complexity and avoids the frequency selectivity for the individual carries. In Fig. 7, 15 appears as a good choice for the number of carriers.

Figure 8 shows the maximum achievable data rate versus the number of carriers for a fixed transmission power. As the number of carriers increases, the power per carrier falls. As long as the power per carrier is adequate for coverage of the area, the data rate increases linearly with an increase in the number of carriers. As the number of carriers increases to the extent that the power of the individual carriers cannot cover the area thoroughly, the linear relation between the data rate and the number of carriers does not hold anymore. As shown in Fig. 8, this number in our case is 30 carriers. This figure also suggests that with a reasonable number of carriers the maximum achievable data rate with coded MCM is 1.5 times more than that of MCM without coding.

Equalization and diversity combining are two of the most popular anti-multipath techniques used for various radio channels. Similar to MCM, and in contrast with spread spectrum technology, equalization and diversity combining provide diversity in the received signal without sacrificing the bandwidth. The DFE is the most popular equalization technique adopted in various radio channels and it takes advantage of the inband time-diversity of the received signal. The SAS is the most

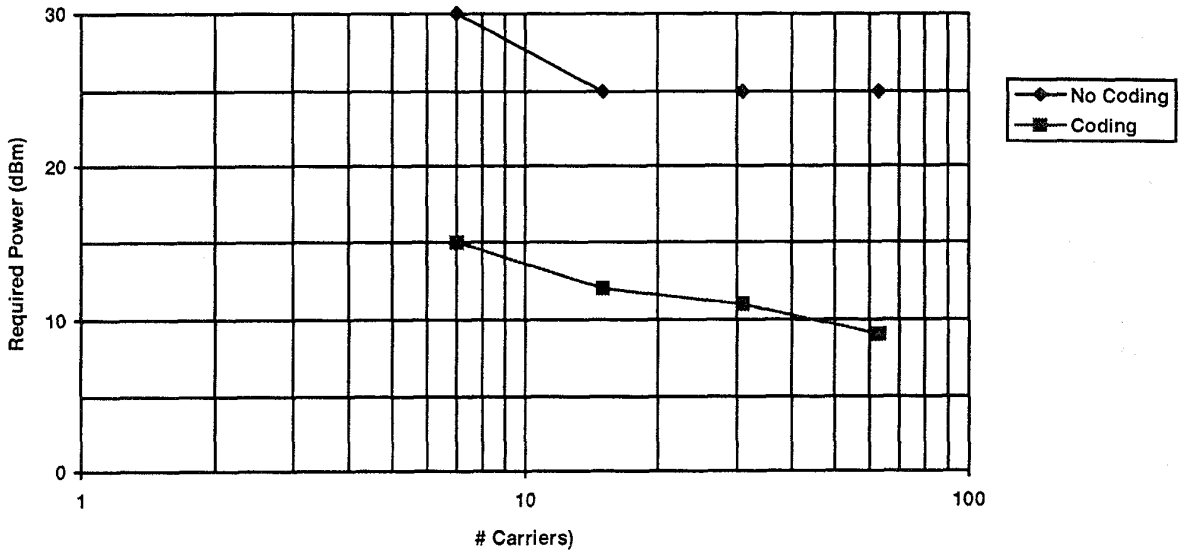

Fig. 7. Multicarrier modulation in a bandlimited channel; 25 MHz, $P_{\text{out}} = 10^{-2}$.

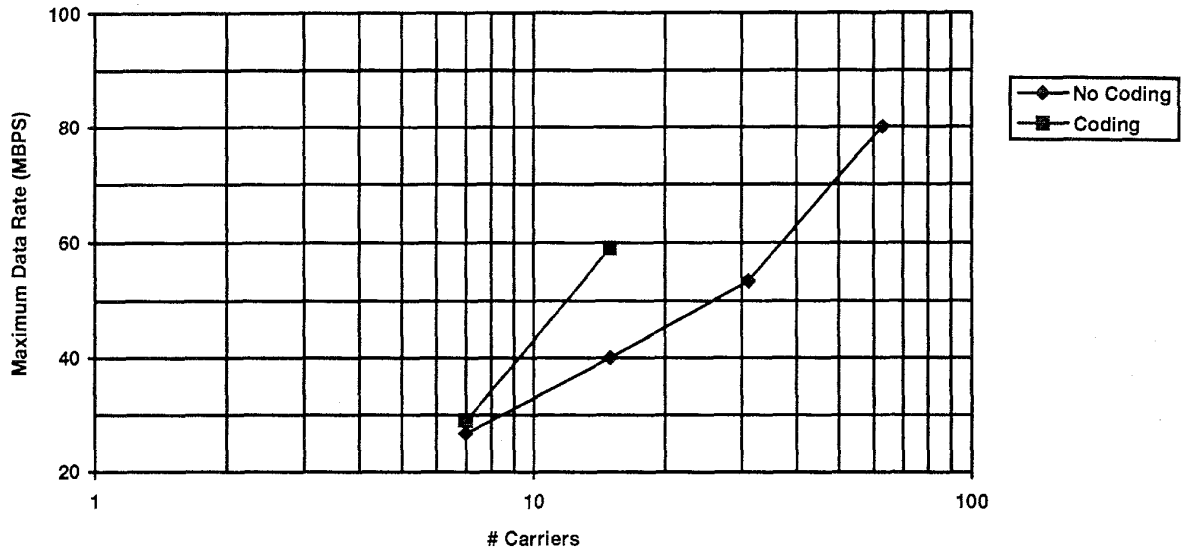

Fig. 8. Multicarrier modulation in a power-limited channel; 100 mW, $P_{\text{out}} = 10^{-2}$.

popular antenna diversity technique that is used in WLAN's. The received signals from different spatial directions are isolated to reduce the negative impact of the multipath arrival of the received signal. The question is what is the maximum data rate that one can achieve if these techniques are adopted in a radio LAN operating in a typical indoor area. The performance of these systems in the area used as the test floor for our performance evaluations was first reported in [42]. Fig. 9 shows the outage probability of systems with sectored antennas, with and without DFE as a function of data rate. As shown in this figure, no combination of sectored antenna systems and decision feedback equalization will provide an outage rate of less than 0.01 in a 25 MHz system bandwidth. Therefore, for a fair comparison among all techniques we should resort to narrower bandwidths.

C. Comparative Performance Analysis in the Test Area

In this section, we compare the bandwidth and power requirements of various transmission techniques operating in the test area. We will also examine the relation of these two requirements to the maximum data rate of each technique. First, we assume a fixed bandwidth of 10 MHz that is considered for the unlicensed operation in the PCS bands, and we compare the minimum required radiation power for all transmission techniques to cover the test area. This part will address the important issue of power consumption for battery oriented applications that are playing a major role in the future market of the WLAN industry. As a part of this discussion, we show that with a maximum transmission power of 100 mW all the transmission techniques discussed in this paper are

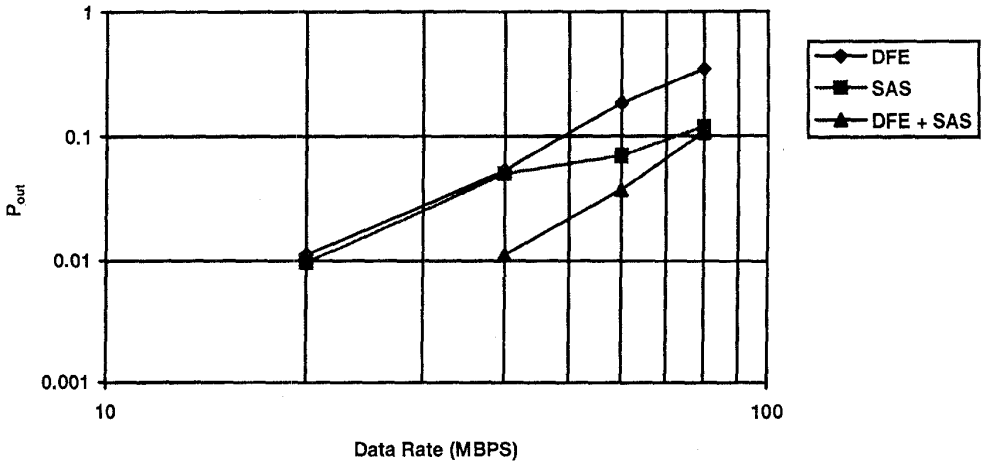

Fig. 9. P_{out} versus bandwidth for DFE, SAS, and DFE/SAS systems, 100 mW.

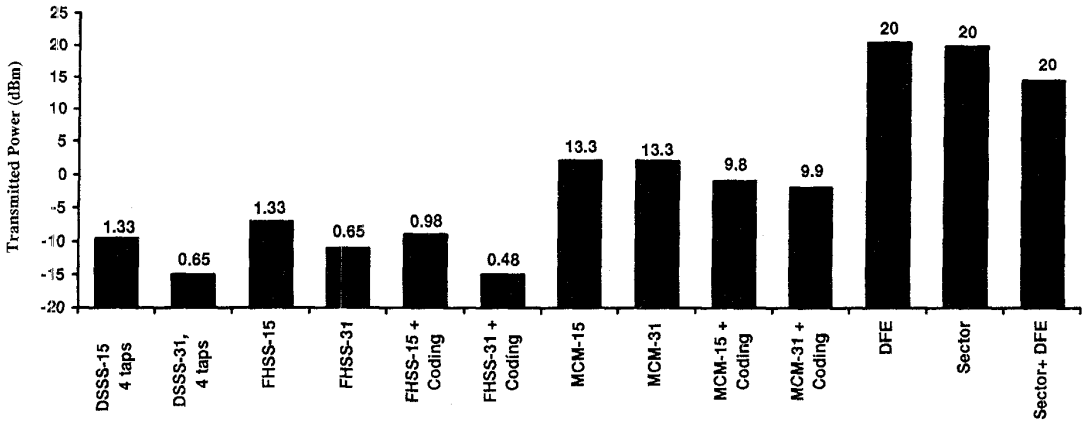

Fig. 10. Minimum power requirements for different transmission techniques, 10 MHz system bandwidth.

able to cover our test area. Then, we assume the transmission power is maintained at 100 mW and there is no restriction on the bandwidth, to determine the maximum data rate that can be achieved with any of the above transmission techniques in the test area. This exercise will address the transmission technologies in the context of demand for higher data rate that has been an extremely important factor in the evolution of the LAN industry. The results can be used as a guideline for the WLAN industry when they approach the frequency administration agencies.

Figure 10 shows the minimum radiation power required to achieve an outage rate of 0.01 in the test area for DSSS with a four-tap RAKE receiver and processing gains of 15 and 31, as well as FHSS and MCM with and without Reed–Solomon coding using 15 and 31 carriers. Also presented are the power requirements to achieve the same outage probability using DFE with three forward and three feedback taps, six sectored SAS and DFE/SAS systems. The total available bandwidth was reduced to 10 MHz in order to accommodate the DFE, SAS, and DFE/SAS systems. Fig. 11 presents similar results for a 25 MHz bandwidth; as discussed earlier, DFE and SAS cannot provide an acceptable performance in that wide of a bandwidth. It should also be noted that the data rate supported by each technique is different. The numbers on the top of bars in Figs. 10 and 11 represent the corresponding data rate for each modulation technique. For the spread spectrum systems, with QPSK modulation and a total system bandwidth of 10 MHz, we have data rates of 1.33 and 0.65 Mb/s for processing gains of 15 and 31, respectively. If coding is used in the FHSS system, these data rates will be lowered to 1 and 0.5 Mb/s. In this bandwidth the data rate for MCM is 13 Mb/s without channel coding and 10 MB/s with channel coding. The data rate for the DFE, SAS, and DFE/SAS is 20 Mb/s, i.e., the maximum among all systems considered. The maximum power consumption of 100 mW (20 dBm) is needed for the DFE and SAS. The DFE/SAS system requires around 15 dBm. Multicarrier modems, regardless of the number of frequencies, operate with around 0 dBm power that requires two orders of magnitude less power than the DFE or SAS. If the MCM uses coding, its power consumption is reduced by about 2–3 dB.

According to results from the test area (shown in Fig. 10), spread spectrum can add between 30 and 35 dB to the fade margin that increases the coverage of the system significantly. DSSS with a four-tap RAKE receiver performs about 2 dB better than FHSS without coding. The RAKE receiver provides a means to exploit the implicit (inband) time-diversity in

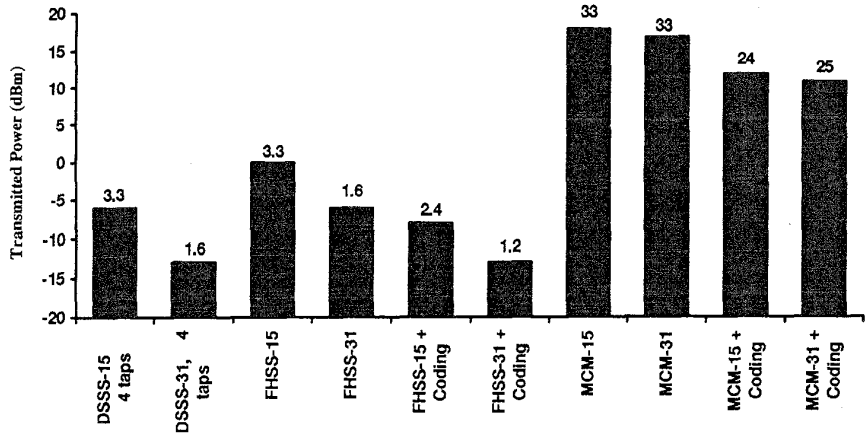

Fig. 11. Minimum power requirements for different transmission techniques, 25 MHz system bandwidth.

the received signal, but the FHSS does not have any such means. Adding coding to the FHSS system, implicit frequency-diversity is exploited by the system and the required radiated powers in the two forms of spread spectrum become very close to one another. The power savings possible with spread spectrum modulation can only be achieved at the expense of data rate. Multicarrier modulation can provide an improvement of about 20–25 dB, with only a small reduction in the data rate.

The quantitative study of radiated power consumption is important for two reasons: 1) Given the restriction on the maximum radiated power by a frequency administration agency, we need to know how the coverage of various transmission techniques compare with one another; 2) considering the increasing expansion of the market for battery operated PCMCIA WLAN's, we need to examine the total power consumption of a modem. The results of Fig. 10 can be used directly to analyze the coverage of various transmission techniques in a typical indoor area. This allows a designer or a standards regulator to justify the selection of a particular transmission technique for a specified system description. Since the power consumption varies substantially with the design and fabrication technology used in the implementation of a WLAN, the designer should use the results of Fig. 10 with their estimation of the electronic power consumption for their own implementation of the system.

Figure 12 presents the maximum attainable data rate for different transmission techniques in the test area. The transmission power is maintained at 100 mW and there is no constraint on the bandwidth used. In each case, the required bandwidth is written on top of the bar graph. A multicarrier modem with 15 carriers can achieve data rates close to 40 Mb/s, and this data rate is doubled when coding is added to the system. With seven carriers, the data rate drops to slightly more than half of the data rate for a 15-carrier system and coding is not as effective as before. The significant difference between the seven carrier and 15-carrier performance reflects the fact that the seven carrier modem operates in a frequency selective fading channel. By appropriate selection of the bandwidth of the individual carrier one may completely eliminate the effects of multipath fading for the system. As a result, if there is no power or bandwidth constraint one can achieve any data rate with multicarrier modems. This property is not shared among other techniques where the increase of data rate finally reaches a point where the effects of frequency selectivity of the channel are dominant and an increase in the transmission power is no longer effective. The restriction in MCM is implementation complexity that increases with an increase in the number of carriers. In practice, however, power and bandwidth are always limited and the implementation complexity is on top of the agenda that has prevented MCM for many wired [56] and wireless applications [32].

As expected, spread spectrum provides lower data rates. However, bandwidth efficiency is only one side of the equation; the processing gain that spread spectrum provides can serve to increase the fade margin, reducing the transmitter's power requirement. This is an important consideration if the wireless network is being used to connect portable, battery-operated computers. Besides, the results presented here are based on single code spread spectrum that is considered by IEEE 802.11. The overall data rate will be increased if we assign several codes to individual users in a CDMA format. Then each spread spectrum channel acts analogous to a carrier in MCM. Similar to MCM, a CDMA modem of this form has limitations caused by the hardware complexity.

The DFE modem has the advantage of having a single channel and it can achieve data rates on the order of 20 Mb/s, as considered for HIPERLAN. Similar results are obtained for sectored antenna systems. However, the complexity of the system for mobile applications has prevented RES-10 from adopting SAS for HIPERLAN [19]. Higher data rates on the order of 30 Mb/s are obtained from the DFE/SAS combination at the expense of a very complex implementation.

V. Conclusions

We showed that performance evaluation using the results of ray tracing shows close agreement with results obtained from empirical channel measurement data. We then used the results of ray tracing for comparative performance evaluation of five transmission techniques that are commonly considered for radio LAN's in a typical indoor test area used for LAN extension operation. Operation in bandlimited and power limited channels were examined in different tests. The results of the

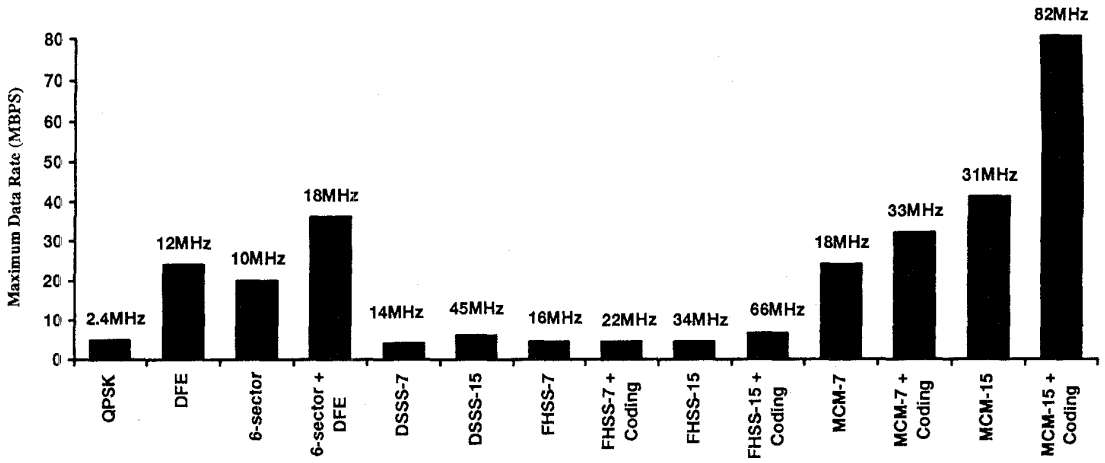

Fig. 12. Maximum attainable data rate for different transmission techniques with no bandwidth restrictions.

test in a bandlimited channel revealed that spread spectrum technology with a processing gain of 15 requires 30–35 dB less radiation power than systems using DFE or SAS which require the maximum radiation power of 100 mW to cover our test area. This ensures a better coverage for the spread spectrum technology, obtained at the expense of a reduction in the data rate supported by the system. To increase the data rate of spread spectrum, single channel CDMA can be adopted. Linear addition of the CDMA channels increases the data rate and the radiation power linearly, and electronic power consumption and the size of the modem nonlinearly. In a power limited channel with 100 mW of transmission power and no restriction on the width of the available frequency band, coded MCM can provide data rates on the order of 80 Mb/s. Increasing the power would allow higher data rates for MCM. In our test area, DFE provides the most bandwidth efficient and practical solution for bandwidths below 12 MHz. The suitability of a technology for a particular application depends on the coverage and data rate requirements as well as allowed complexity and cost of the development. The results of this paper serve as a guideline for the evolving standards and designs to suit an appropriate transmission technique to a WLAN specification.

Appendix
Error Rate Analysis

Since QPSK modulation with coherent detection is assumed, error probability for the I and Q channels can be computed separately, and combined to arrive at a symbol error rate. With the above in mind, the complex decision variables for all of the systems (after phase compensation) can be broken down into their real and imaginary parts, as follows:

$$z(T_d|\{b_i\}) \cdot e^{-j\gamma} \equiv z^I(T_d, \gamma|\{b_i\}) + jz^Q(T_d, \gamma|\{b_i\})$$

where T_d is the sampling time and γ is the phase compensation introduced by the receiver. Note that when a K-tap RAKE receiver is used, the decision variable will be the sum of K complex samples of $z(t)$. The expressions for $z(t)$ for the different modulation techniques were derived earlier. For example, in the case of DSSS with a one-tap receiver, the in-phase and quadrature components of the decision variable can be written as

$$z^I(T_d, \gamma|\{b_i\}) = \sum_i \sum_{l=0}^{L-1} \beta_l \cdot R_x(T_d - iT - \tau_l) \cdot [b_i^I \cdot \cos(\varphi_l - \gamma) - b_i^Q \cdot \sin(\varphi_l - \gamma)] + n^I(T_d)$$

and

$$z^Q(T_d, \gamma|\{b_i\}) = \sum_i \sum_{l=0}^{L-1} \beta_l \cdot R_x(T_d - iT - \tau_l) \cdot [b_i^Q \cdot \cos(\varphi_l - \gamma) + b_i^I \cdot \sin(\varphi_l - \gamma)] + n^Q(T_d)$$

where b_i^I and b_i^Q represent the information bits making up the in-phase and quadrature components of the ith information symbol, b_i

$$b_i \equiv b_i^I + jb_i^Q.$$

Error probabilities in the in-phase and quadrature channels are obtained by averaging the corresponding error probability over the symbol patterns

$$P^I(e|\{b_i\}) = \frac{1}{2} \sum_i P\{b_i\} \cdot \operatorname{erfc}\left[\frac{z_I(T_d, \gamma|\{b_i\})}{\sigma^I}\right]$$

$$P^Q(e|\{b_i\}) = \frac{1}{2} \sum_i P\{b_i\} \cdot \operatorname{erfc}\left[\frac{z_Q(T_d, \gamma|\{b_i\})}{\sigma^Q}\right]$$

where σ^I and σ^Q are the variances of $n^I(t)$ and $n^Q(t)$, respectively. In practice, because of the limited duration of the pulse and channel impulse response, every symbol is only affected by a few neighbors. Without channel coding, the symbol error probability is given by

$$P_S(e) = P^I(e) + P^Q(e) - P^I(e) \cdot P^Q(e).$$

The relationship between symbol errors and bit errors depends on the mapping of the two information bits onto the QPSK symbol. If a Gray Code is used, in which 2-b groups assigned

to adjacent symbols differ by only one bit, the bit error probability can be approximated as

$$P_b(e) \approx \frac{P_S(e)}{2}.$$

The receiver's front-end noise was computed following the derivation in [57]. At an operating temperature of 290 K, thermal noise will be -174 dBm/Hz. In the case of DSSS, the bandwidth of the front-end filter is 25 MHz, resulting in noise variance of -100 dBm. In frequency hopping and multicarrier modulation, the front-end filter's bandwidth is dependent on the data rate (data rate per channel in the case of MCM), resulting in a higher noise variance at higher data rates.

In both frequency hopping and multicarrier modulation, different information bits are transmitted on different carriers, and (given sufficient frequency separation between the carriers) will be subject to statistically independent fading. As a result, it is possible to combat the effect of frequency-selective fading using channel coding techniques [58]. In this paper, the effect of Reed–Solomon coding, when used in conjunction with slow frequency hopping or multicarrier modulation is also studied. The number of bits in a channel codeword are set equal to the number of carriers, so that one bit from a channel codeword will be transmitted on each carrier. When studying systems with 7, 15, 31, and 63 carriers, Reed–Solomon codes of (7, 5), (15, 11), (31, 23), and (63, 45) are assumed, resulting in an approximately 27% reduction in data rate due to coding.

The error rate calculations closely follow the derivations in [59, Appendix 1]. In an n-carrier system, let the error probability on the ith carrier be p_i. Defining the following variables:

$$s_i \equiv \frac{p_i}{1-p_i}$$

and

$$S_j \equiv \sum_{i=0}^{n-1} (s_i)^j.$$

Let P_u be the probability that exactly u bits are received in error. Then

$$P_u = \begin{cases} \prod_{i=1}^{n} (1-p_i), & \text{for } u = 0 \\ \frac{1}{u} \sum_{i=1}^{u} (-1)^{i-1} \cdot S_i \cdot P_{t-i}, & \text{for } u \geq 1. \end{cases}$$

If the coding scheme can correct up to $t = (n-k)/2$ errors, the probability of an uncorrectable codeword error is given by

$$P_{ce} = \sum_{u=t+1}^{n} P_u.$$

REFERENCES

[1] K. Pahlavan, "Wireless communication for office information networks," *IEEE Commun. Mag.*, vol. 23, pp. 19–27, June 1985.

[2] ——, "Wireless intraoffice networks," *ACM Trans. Office Inform. Syst.*, vol. 6, pp. 277–303, July 1988.

[3] K. Pahlavan and A. Levesque, "Wireless data communications," *IEEE Proc.*, vol. 82, pp. 1398–1430, Sept. 1994.

[4] K. Pahlavan, T. Probert, and M. Chase, "Trends in local wireless networks," *IEEE Commun. Mag.*, vol. 33, pp. 88–95, Mar. 1995.

[5] F. Gfeller and U. Bapst, "Wireless in-house data communication via diffuse infrared radiation," *IEEE Proc.*, vol. 67, pp. 1474–1486, Nov. 1979.

[6] P. Ferert, "Application of spread spectrum radio to wireless terminal communications," in *Proc. NTC,* Houston, TX, Dec. 1980, pp. 244–248.

[7] M. J. Marcus, "Recent US regulatory decisions on civil uses of spread spectrum," in *Proc. IEEE GLOBECOMM,* 1985, pp. 16.6.1–16.6.3.

[8] M. Marcus, "Regulatory policy considerations for radio local area networks," *IEEE Commun. Mag.*, vol. 25, pp. 95–99, July 1987.

[9] ——, "Regulatory policy considerations for radio local area networks," in *Proc. IEEE Workshop on Wireless LAN's,* Worcester, MA, May 1991, pp. 42–48.

[10] T. A. Freeburg, "Enabling technologies for wireless in-building network communications—Four technical challenges, four solutions," *IEEE Commun. Mag.*, vol. 29, pp. 58–64, Apr. 1991.

[11] T. Freeburg, "A new technology for high speed wireless local area networks," in *IEEE Workshop on Wireless Local Area Networks,* Worcester, MA, May 1991, pp. 127–139.

[12] B. Tuch, "An ISM band spread spectrum locan area network: WaveLAN," in *IEEE Workshop on Wireless Local Area Networks,* Worcester, MA, May 1991, pp. 103–111.

[13] J. Barry, J. Kahn, E. Lee, and D. Messerschmitt, "High-speed nondirective optical communication for wireless networks," *IEEE Network Mag.*, vol. 29, pp. 44–54, Nov. 1991.

[14] *Proc. IEEE Workshop on Wireless Local Area Networks,* Worcester, MA, May 1991.

[15] V. Hayes, "Wireless LANs—Standard activities in IEEE," in *Proc. IEEE Workshop on Wireless LAN's,* Worcester, MA, May 1991, pp. 57–63.

[16] ——, "Standardization efforts for wireless LAN's," *IEEE Network Mag.*, vol. 29, pp. 19–20, Nov. 1991.

[17] ——, "Radio-LAN standardization efforts," in *Proc. IEEE Conf. Wireless LAN Implementation,* Dayton, OH, 1992, pp. 1–4.

[18] A. Nix, M. Li, J. Marvill, T. Wilkinson, I. Johnson, and S. Barton, "Modulation and equalization considerations for high performance radio LAN's (HIPERLAN)," in *IEEE Int. Symp. Personal, Indoor, and Mobile Radio Communications,* Hague, The Netherlands, Sept. 1994, pp. 964–968.

[19] T. A. Wilkinson, T. Phipps, and S. K. Barton, "A report on HIPERLAN standardization," *Int. J. Wireless Inform. Networks,* vol. 2, pp. 99–120, Mar. 1995.

[20] T. Wilkinson and A. Jones, "Minimization of the peak to mean envelope power ratio of multicarrier transmission schemes by block coding," in *IEEE 45th Veh. Technol. Conf.*, Chicago, IL, July 1995, pp. 825–829.

[21] T. S. Rappaport, "The wireless revolution," *IEEE Commun. Mag.*, vol. 29, pp. 52–71, Nov. 1991.

[22] J. Cheah, "A proposed access method for the wireless LAN standard," in *IEEE Int. Symp. PIMRC,* Boston, MA, Oct. 1992, pp. 145–148.

[23] R. Caceres and L. Iftode, "Improving the performance of reliable transport protocols in mobile computing environments," *IEEE J. Select. Areas Commun.*, vol. 13, pp. 850–857, June 1995.

[24] A. Myles, D. Johnson, and C. Perkins, "A mobile host protocol supporting route optimization and authentication," *IEEE J. Select. Areas Commun.*, vol. 13, pp. 839–849, June 1995.

[25] D. Duchamp, "Issues in wireless mobile computing," in *3rd IEEE Workshop on Workstation Operating Systems,* Key Biscayne, FL, Apr. 1992, pp. 2–10.

[26] *IEEE Personal Communications,* special Issue on Security in Wireless Systems, vol. 2, no. 4, Aug. 1995.

[27] G. Turin *et al.*, "A statistical model of urban multipath propagation," *IEEE Trans. Veh. Technol.*, vol. VT-21, pp. 1–9, Feb. 1972.

[28] A. Saleh and R. Valenzuela, "A statistical model for indoor multipath propagation," *IEEE J. Select. Areas Commun.*, vol. SAC-5, pp. 128–137, Feb. 1987.

[29] R. Ganesh and K. Pahlavan, "Statistical modeling and computer simulation of indoor radio channel," *IEE Proc.*, vol. 138, pp. 153–161, June 1991.

[30] T. S. Rappaport, "Statistical channel impulse response models for factory and open plan building radio communication system design," *IEEE Trans. Commun.*, vol. 39, pp. 794–806, May 1991.

[31] H. Hashemi, "The indoor radio propagation channel," *Proc. IEEE,* vol. 18, pp. 943–968, July 1993.

[32] K. Pahlavan and A. Levesque, *Wireless Information Networks.* New York: Wiley, 1995.

[33] S. Howard and K. Pahlavan, "Performance of adaptive equalization over measured indoor radio channels," *IEEE Electron. Lett.,* Sept. 1989.

[34] K. Pahlavan, S. Howard, and T. Sexton, "Decision feedback equalization of the indoor radio channel," *IEEE Trans. Commun.*, vol. 41, pp. 164–170, Jan. 1993.

[35] M. Chase and K. Pahlavan, "Performance of DS-CDMA over measured indoor radio channels using random orthogonal codes," *IEEE Trans. Veh. Technol.,* vol. 42, pp. 617–624, Nov. 1993.
[36] M. Kavehrad and B. Ramamurthi, "Direct sequence spread spectrum with DPSK modulation and diversity for indoor wireless communications," *IEEE Trans. Commun.,* vol. COM-35, pp. 224–236, Feb. 1987.
[37] S. Howard and K. Pahlavan, "Frequency domain characterization of indoor radio channels," *IEEE Trans. Instrumen. Meas.,* vol. 39, pp. 751–755, Oct. 1990.
[38] Joint Technical Committee of Committee T1 R1p1.4 and TIA R46.3.3/TR 45.4.4 on Wireless Access, "Draft final report on RF channel characterization," Paper no. JTC (AIR)/94.01.17-238r4, Jan. 17, 1994.
[39] R. Valenzuela, "Performance of adaptive equalization for indoor radio communications," *IEEE Trans. Commun.,* vol. 37, pp. 291–293, Mar. 1989.
[40] T. Sexton and K. Pahlavan, "Channel modeling and adaptive equalization of indoor radio channels," *IEEE J. Select. Areas Commun.,* vol. 7, pp. 114–121, Jan. 1989.
[41] S. Seidel and T. Rappaport, "Site-specific propagation prediction for wireless in-building personal communication system design," *IEEE Trans. Veh. Technol.,* vol. 43, pp. 879–891, Nov. 1994.
[42] G. Yang, K. Pahlavan, and T. Holt, "Sector antenna and DFE modems for high speed indoor radio communications," *IEEE Trans. Veh. Technol.,* vol. 43, pp. 925–933, Nov. 1994.
[43] J. McKown and R. Hamilton, Jr., "Ray tracing as a design tool for radio networks," *IEEE Network Mag.,* pp. 27–30, Nov. 1991.
[44] M. Lebherz, W. Wiesbeck, and W. Krank, "A versatile wave propagation model for the VHF/UHF range considering three-dimensional terrain," *IEEE Trans. Antennas Propagat.,* vol. 40, pp. 1121–1131, Oct. 1992.
[45] T. S. Rappaport and D. A. Hawbaker, "A ray tracing technique to predict path loss and delay spread inside buildings," in *IEEE GLOBECOM '92,* Orlando, FL, Dec. 1992, pp. 649–653.
[46] T. Holt, K. Pahlavan, and J. F. Lee, "A graphical indoor radio channel simulator using 2D ray tracing," in *IEEE PIMRC'92,* Boston, MA, Oct. 1992, pp. 411–416.
[47] R. Valenzuela, "A ray tracing approach to predicting indoor wireless transmission," in *IEEE 43rd Veh. Technol. Conf.,* Secaucus, NJ, May 1993, pp. 214–218.
[48] G. Yang, "Performance evaluation of high speed wireless data systems using a 3D ray tracing algorithm," Ph.D. dissertation, Worcester Polytechnic Institute, Worcester, MA, June 1994.
[49] R. Valenzuela, "Performance of quadrature amplitude modulation for indoor radio communications," *IEEE Trans. Commun.,* vol. COM-35, pp. 1236–1238, Nov. 1987.
[50] K. Pahlavan, "Comparison between the performance of QPSK, SQPSK, QPR, and SQPR systems over microwave LOS channels," *IEEE Trans. Commun.,* vol. COMM-33, pp. 291–296, Mar. 1985.
[51] L. Cimini, "Analysis and simulation of a digital mobile channel using orthogonal frequency division multiplexing," *IEEE Trans. Commun.,* vol. COMM-33, pp. 665–675, July 1985.
[52] C. L. Despins, D. D. Falconer, and S. A. Mahmoud, "Compound strategies of coding, equalization, and space diversity for wideband TDMA indoor wireless channels," *IEEE Trans. Veh. Technol.,* vol. 41, pp. 369–379, Oct. 1992.
[53] S. Hara *et al.,* "Multicarrier modulation technique for broadband indoor wireless communications," in *IEEE Int. Symp. PIMRC,* Yokohama, Japan, Sept. 1993.
[54] G. Yang and K. Pahlavan, "Performance analysis of multicarrier modems in an office environment using 3D ray tracing," in *IEEE GLOBECOM '94,* San Francisco, CA, Nov. 1994, pp. 42–46.
[55] R. J. C. Bultitude, "Measurement, characterization, and modeling of indoor 800/900 MHz radio channels for digital communications," *IEEE Commun. Mag.,* vol. 25, pp. 5–12, June 1987.
[56] K. Pahlavan and J. L. Holsinger, "Voice-band data communication modems a historical review: 1919–1988," *IEEE Commun. Mag.,* vol. 26, pp. 16–27, Jan. 1988.
[57] W. C. Y. Lee, *Mobile Cellular Telecomm. Systems.* New York: McGraw-Hill, 1989.
[58] J. Proakis, *Digital Communications,* 2nd ed. New York: McGraw-Hill, 1989.
[59] M. Pursley and S. Sandberg, "Variable-rate coding for meteor-burst communications," *IEEE Trans. Commun.,* vol. 37, pp. 1105–1112, Nov. 1989.

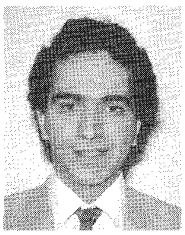

Aram Falsafi was born in Tehran, Iran, in 1965. He received the B.S. degree from Worcester Polytechnic Institute, Worcester, MA, in 1986, and the M.S. degree from Rensselaer Polytechnic Institute, Troy, NY, in 1988, both in electrical engineering.

From 1988 to 1994, he was with Digital Equipment Corporation, working on graphical user interfaces for data acquisition, instrument control, and signal processing. He is currently completing the Ph.D. degree in electrical engineering at Worcester Polytechnic Institute. He spent the summer of 1995 at GTE Labs, developing a graphical user interface for propagation modeling software. His research interests are in indoor radio propagation modeling, performance analysis of wireless transmission techniques, and user interface design. He is also a volunteer coordinator for TecsChange, a Boston-based organization promoting responsible technology transfer to the developing world.

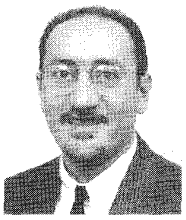

Kaveh Pahlavan (M'79–SM'88–F'95) received the Ph.D. degree in electrical engineering from Worcester Polytechnic Institute, Worcester, MA.

He started his career as an Assistant Professor at Northeastern University, Boston, MA. Currently, he is the Weston Hadden Professor of Electrical and Computer Engineering and the director of the Center for Wireless Information Network Studies (CWINS) at the Worcester Polytechnic Institute, Worcester, MA. Before joining WPI, he was the director of advanced development at Infinite Inc., Andover, MA, working on voice band data communications. For the past decade, his basic research has been focused on indoor radio propagation modeling and analysis of the multiple access and transmission methods for wireless local area networks. His previous research background is on modulation, coding, and adaptive signal processing for digital communication over voice-band and fading multipath radio channels. He has contributed to more than 100 technical papers and five book chapters, has presented numerous tutorials and short courses in 10 different countries, and has been a consultant to many industries including GTE Laboratories, Steinbrecher Corp., DEC, WINDATA, Honeywell, BBN, and Codex. Results of his research work at CWINS constitutes the main parts of his textbook, *Wireless Information Networks* (New York: Wiley 1995, co-authored by A. Levesque). He is the Editor-in-Chief of the *International Journal on Wireless Information Networks.*

Dr. Pahlavan was the program chairman and organizer of the IEEE Wireless LAN Workshop, Worcester, MA, May 9–10, 1991 and the organizer and the technical program chairman of the Third IEEE International Symposium on Personal, Indoor, and Mobile Radio Communications, Boston, MA, October 19–21, 1992. He is a member of Eta Kappa Nu.

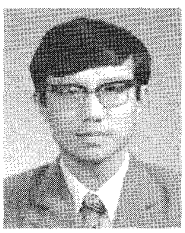

Ganning Yang (S'94–M'95) was born in Nanjing, China, on April 6, 1963. He received the B.S. and M.S. degrees from the University of Science and Technology of China, Hufei, China, in 1986 and 1989, and the Ph.D. degree from Worcester Polytechnic Institute, Worcester, MA, in 1994, respectively, all in electrical engineering.

Following graduation, he joined Rockwell International Corporation's Wireless Communications Division to begin work on wireless communication systems development. He is currently involved in system architecture design and analysis for PCS and cordless products. His research interests are in performance analysis of wireless communication systems, radio propagation, and channel modeling in indoor or mobile radio channels.